Supporting Information for the paper:

Structure-Reactivity Correlations in Metal Atom Substitutions of Monolayer-Protected Noble Metal Alloy Clusters

Kumaranchira Ramankutty Krishnadas, Debasmita Ghosh, Atanu Ghosh, Ganapati Natarajan

*and Thalappil Pradeep**

Department of Chemistry, DST Unit of Nanoscience (DST UNS) and Thematic Unit of Excellence (TUE)
Indian Institute of Technology Madras
Chennai 600 036, India
E-mail: pradeep@iitm.ac.in

General instrumental parameters used for ESI measurements

All samples were analyzed by Waters Synapt G2Si High Definition Mass Spectrometer equipped with electrospray ionization (ESI) and ion mobility (IM) separation. All the samples were analyzed in negative ESI mode. The optimized conditions for each experiments were as follows:

Characterization and reactions of $Au_{25-x}Ag_x(SR)_{18}$

Sample concentration: 10 µg /mL

Diluent: DCM

Sample flow rate: 20-30 µL/min

Source voltage: 2-3 kV

Cone voltage: 120-140 V

Source offset: 80-120 V

Trap collision Energy: 0 V

Transfer collision Energy: 0 V

Source temperature: 100°C

Desolvation temperature: 150°C

Desolvation gas Flow: 400 L/h

Characterization and reactions of $Ag_{25-x}Au_x(SR)_{18}$

Sample concentration: 10 µg /mL

Diluent: DCM

Sample flow rate: 20-30 µL/min

Source voltage: 1-2 kV

Cone voltage: 30-50 V

Source offset: 30 V

Trap collision Energy: 0 V

Transfer collision Energy: 0 V

Sourcet: 100°C

Desolvation temperature: 150°C

Desolvation gas Flow: 400 L/h

Characterization and reactions of $Au_xAg_{44-x}(SR)_{30}$

Sample concentration: 10 µg /mL

Diluents: DCM

Sample flow rate: 20-30 µL/min

Source voltage: 0.5-2 kV

Cone voltage: 30-60 V

Source offset: 30-40 V

Trap collision Energy: 0 V

Transfer collision Energy: 0 V

Source temperature: 100°C

Desolvation temperature: 150°C

Desolvation gas flow: 400 L/h

Table of contents

Supporting Information 1

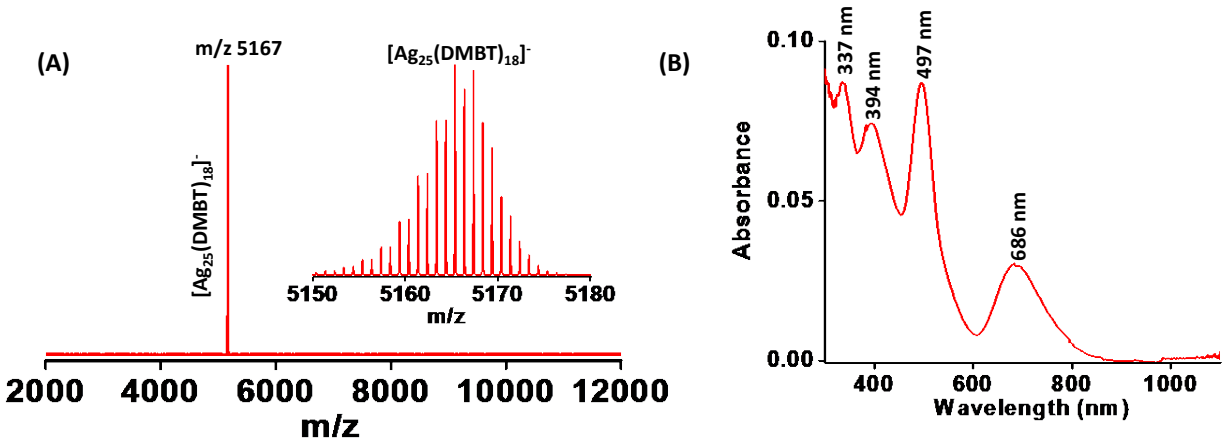

Figure S1. ESI mass spectrum (A) and UV/vis absorption spectrum (B) of $Ag_{25}(DMBT)_{18}$. Characteristic peak positions are marked in each spectrum. Isotopic pattern of $Ag_{25}(DMBT)_{18}$ is shown in the inset of (A).

.

Supporting Information 2

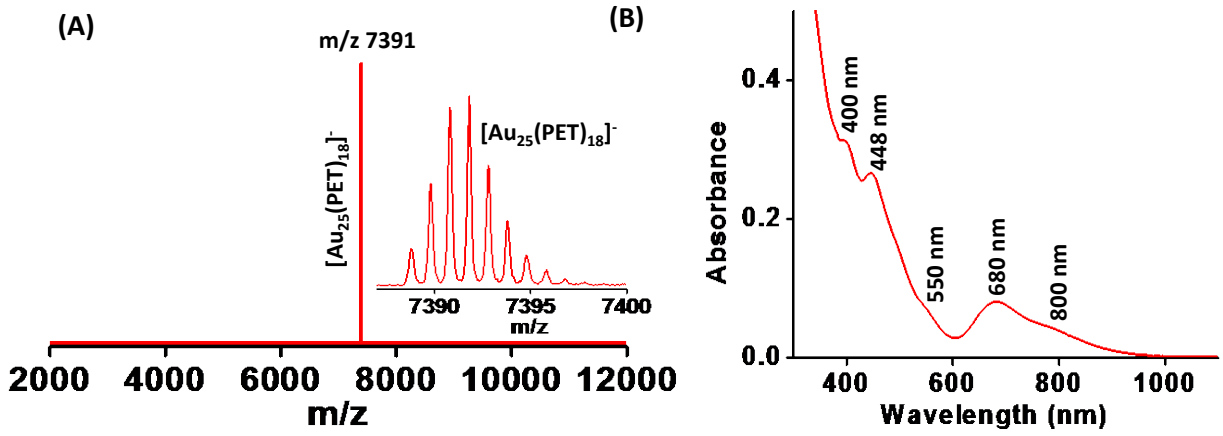

Figure S2. ESI mass spectrum (A) and UV/vis absorption spectrum (B) of $Au_{25}(PET)_{18}$. Characteristic peak positions are marked in each spectrum. Isotopic pattern of $Au_{25}(PET)_{18}$ is shown in the inset of (A).

Supporting Information 3

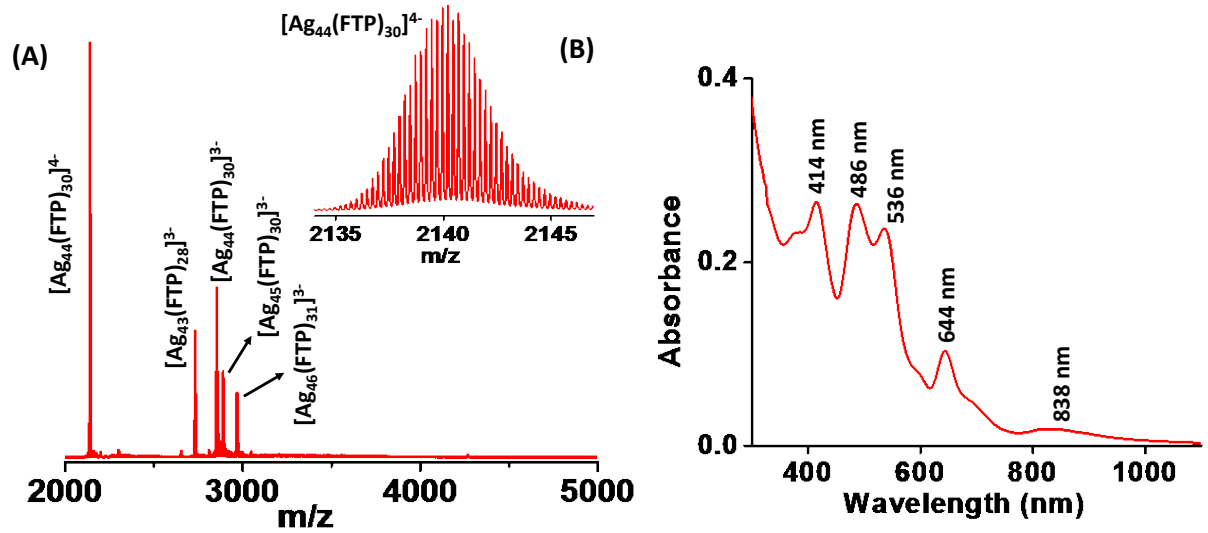

Figure S3. ESI mass spectrum (A) and UV/vis absorption spectrum (B) of $Ag_{44}(FTP)_{30}$. Characteristic peak positions are marked in each spectrum. Isotopic pattern of $[Ag_{44}(FTP)_{30}]^{4-}$ is shown in the inset of (A).

Supporting Information 4

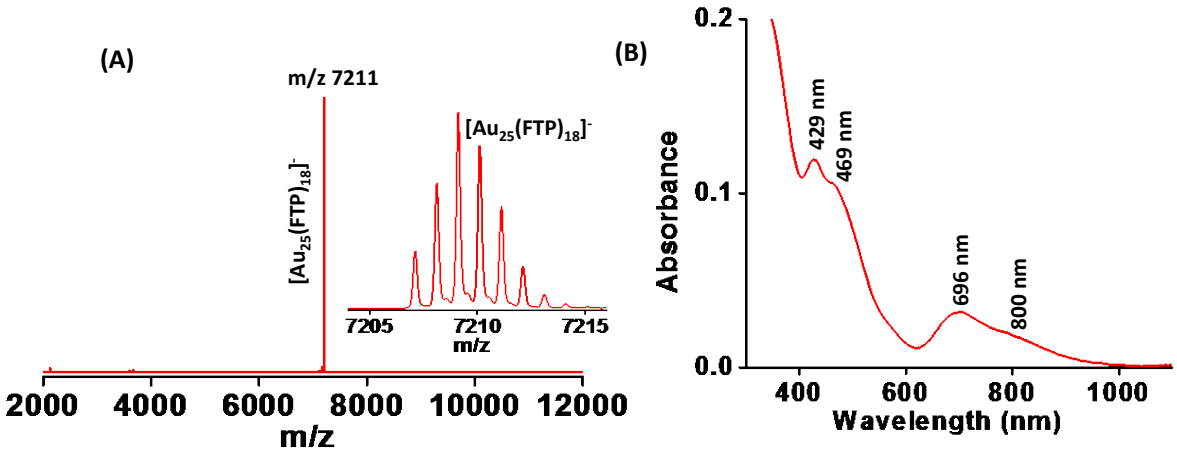

Figure S4. ESI mass spectrum (A) and UV/vis absorption spectrum (B) of $Au_{25}(FTP)_{18}$. Characteristic peak positions are marked in each spectrum. Isotopic pattern of $Au_{25}(FTP)_{18}$ is shown in the inset of (A).

Supporting Information 5

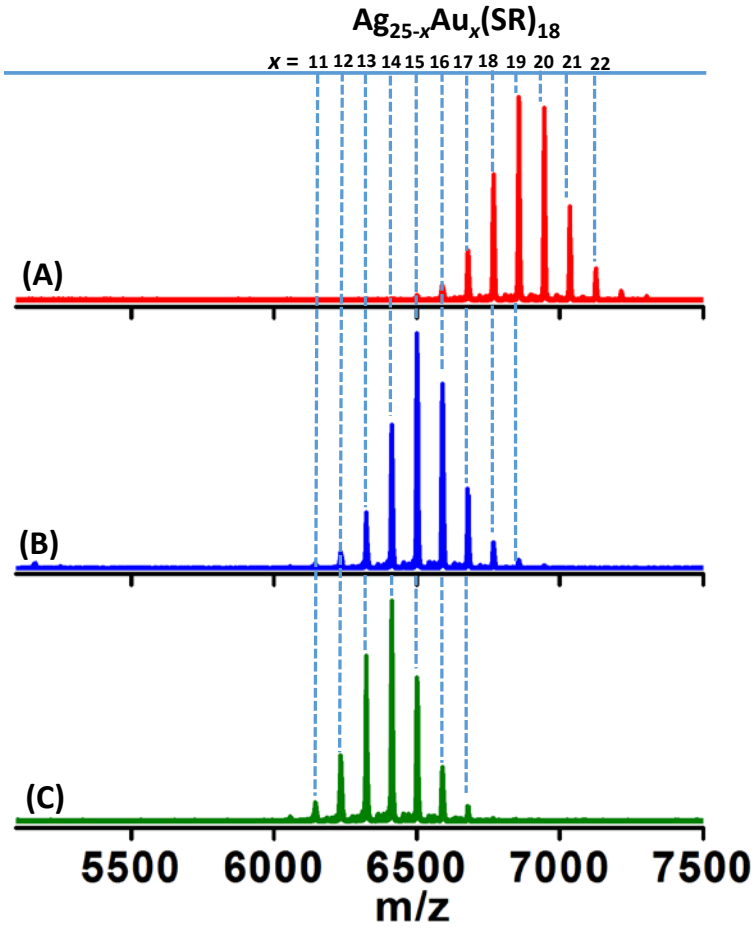

Figure S5. ESI mass spectra of a mixture of $Ag_{25-x}Au_x(SR)_{18}$ with x > 12 before (A), 2 min (B), 20 min (C) after the addition of $Ag_{25}(DMBT)_{18}$ into it.

Supporting Information 6

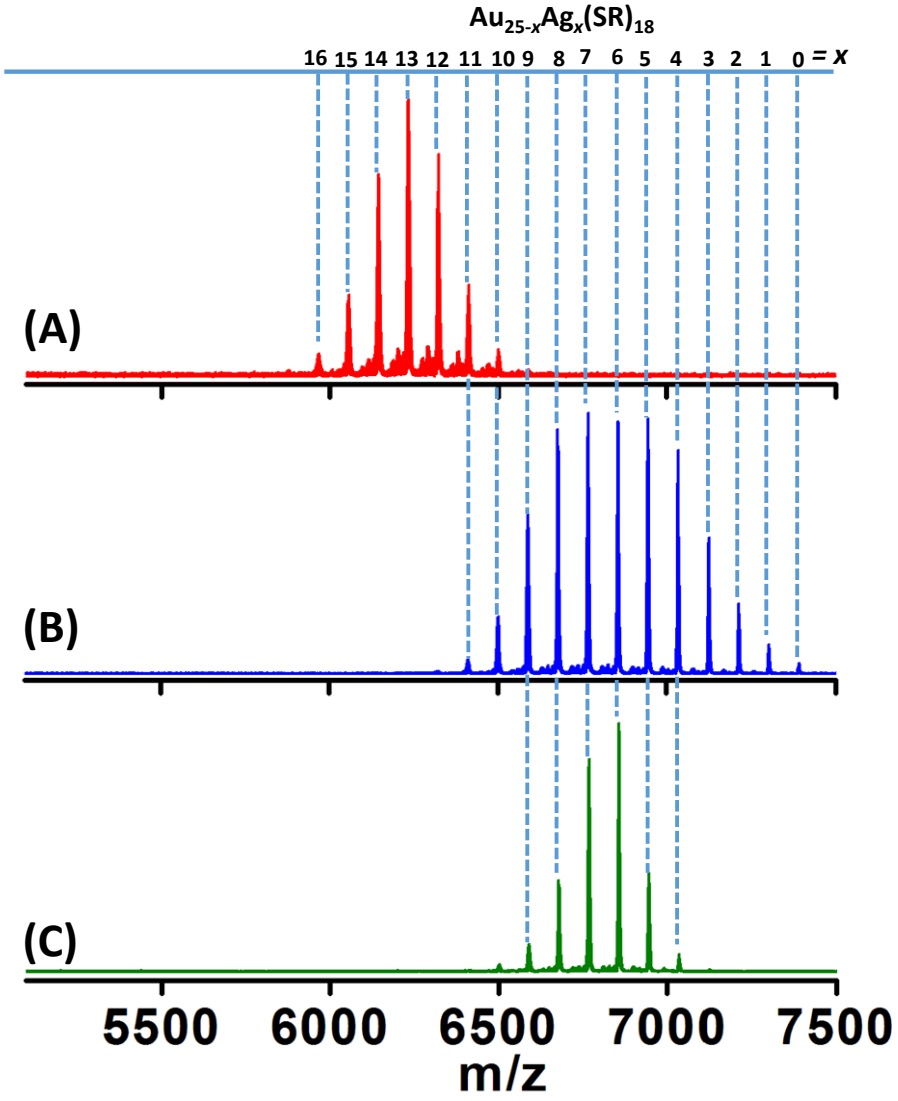

Figure S6. ESI mass spectra of a mixture of $Au_{25-x}Ag_x(SR)_{18}$ with x > 12 before (A), 2 min (B), 5 h (C) after the addition of $Au_{25}(PET)_{18}$ into it.

Supporting Information 7

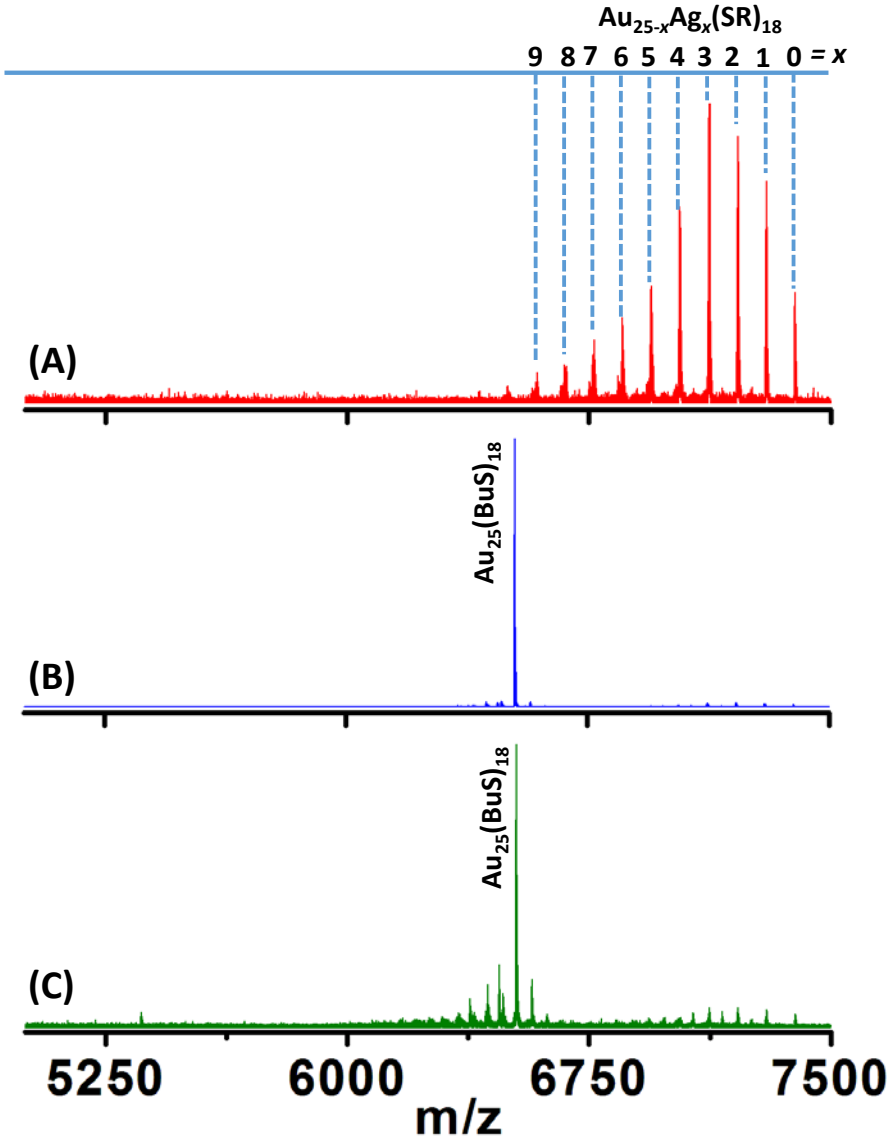

Figure S7. ESI mass spectra of a mixture of $Au_{25-x}Ag_x(SR)_{18}$ with x = 1-10 before (A), 2 min (B), and 1 h (C) after the addition of $Au_{25}(BT)_{18}$ into it.

Supporting Information 8

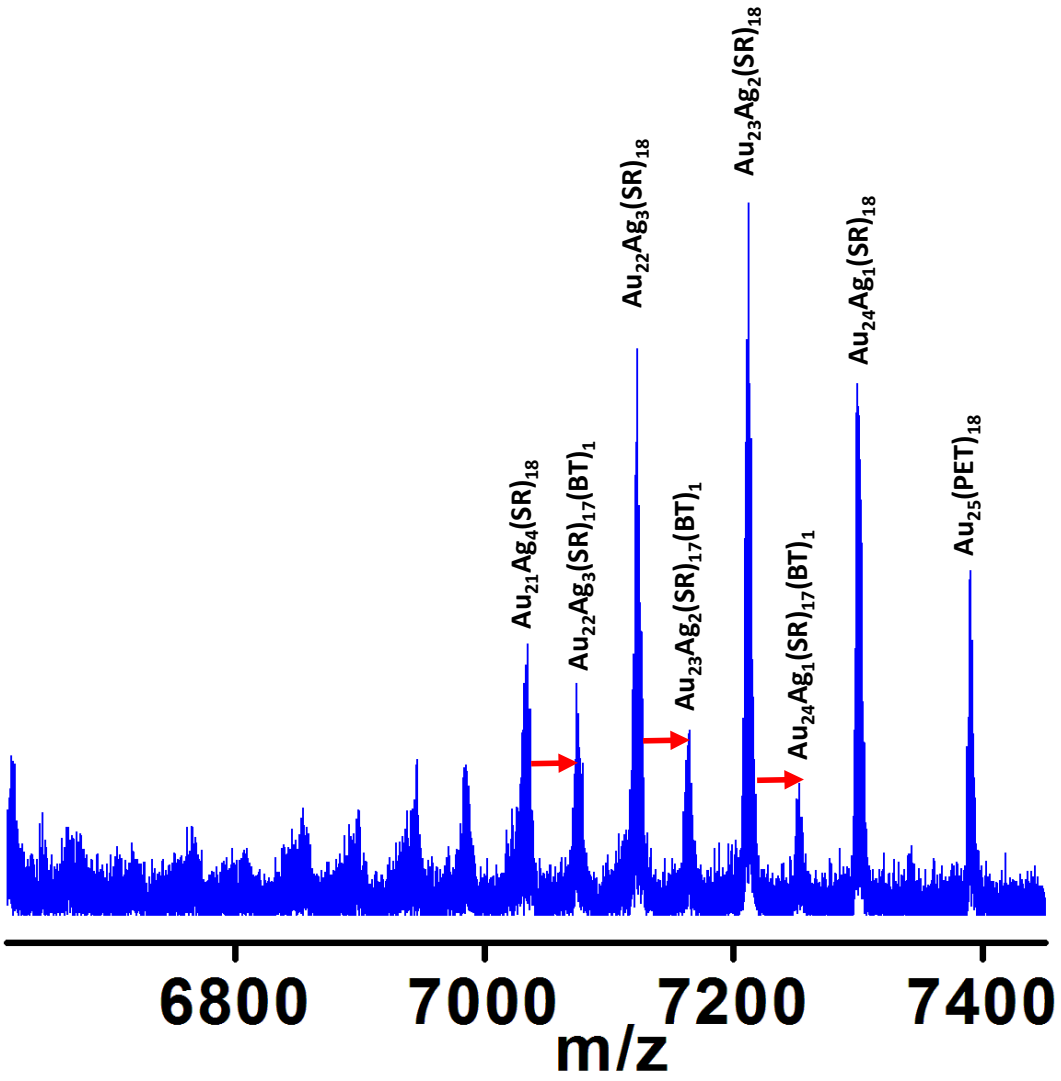

Figure S8. Expansion of the ESI mass spectra shown in Figure S7B showing the mixture of $Au_{25-x}Ag_x(SR)_{18}$ along with the features due to fragment substitution. The red arrows indicate that the clusters $Au_{24}Ag_1(SR)_{17}(BT)_1$, $Au_{23}Ag_2(SR)_{17}(BT)_1$, $Au_{22}Ag_3(SR)_{17}(BT)_1$, *etc.*, are derived from the $Au_{23}Ag_2(SR)_{18}$, $Au_{22}Ag_3(SR)_{18}$ and $Au_{21}Ag_4(SR)_{18,}$ respectively, through metal-ligand exchange, i.e., (Ag-SR)-(Au-BT) exchange. Refer to the note below for details.

Note: The peaks $Au_{24}Ag_1(SR)_{17}(BT)_1$, $Au_{23}Ag_2(SR)_{17}(BT)_1$, $Au_{22}Ag_3(SR)_{17}(BT)_1$, *etc.*, can be considered as derived from ligand exchange of $Au_{24}Ag_1(SR)_{18}$, $Au_{23}Ag_2(SR)_{18}$, $Au_{22}Ag_3(SR)_{18}$, respectively. However, if the former set of peaks (with –SR and BT ligands) are only due to ligand exchange, there should not be any change in the extent of alloying. However,

comparison of Figure S7A and S8 shows that number of Ag atoms present in the parent solution of $Au_{25-x}Ag_x(SR)_{18}$ clusters (see Figure S7A) has reduced from 0-9 to 0-4. This reduction in number of Au atoms cannot be explained by the ligand exchange as it cannot result in the substitution of metal atoms. Therefore, we conclude that the peaks $Au_{24}Ag_1(SR)_{17}(BT)_1$, $Au_{23}Ag_2(SR)_{17}(BT)_1$, $Au_{22}Ag_3(SR)_{17}(BT)_1$, *etc.*, are most likely due to the metal-ligand exchange, i.e., (Ag-SR)-(Au-BT) exchange. However, contribution from the ligand exchange *i.e.*, -SR – BT exchange cannot be ruled out.

Supporting Information 9

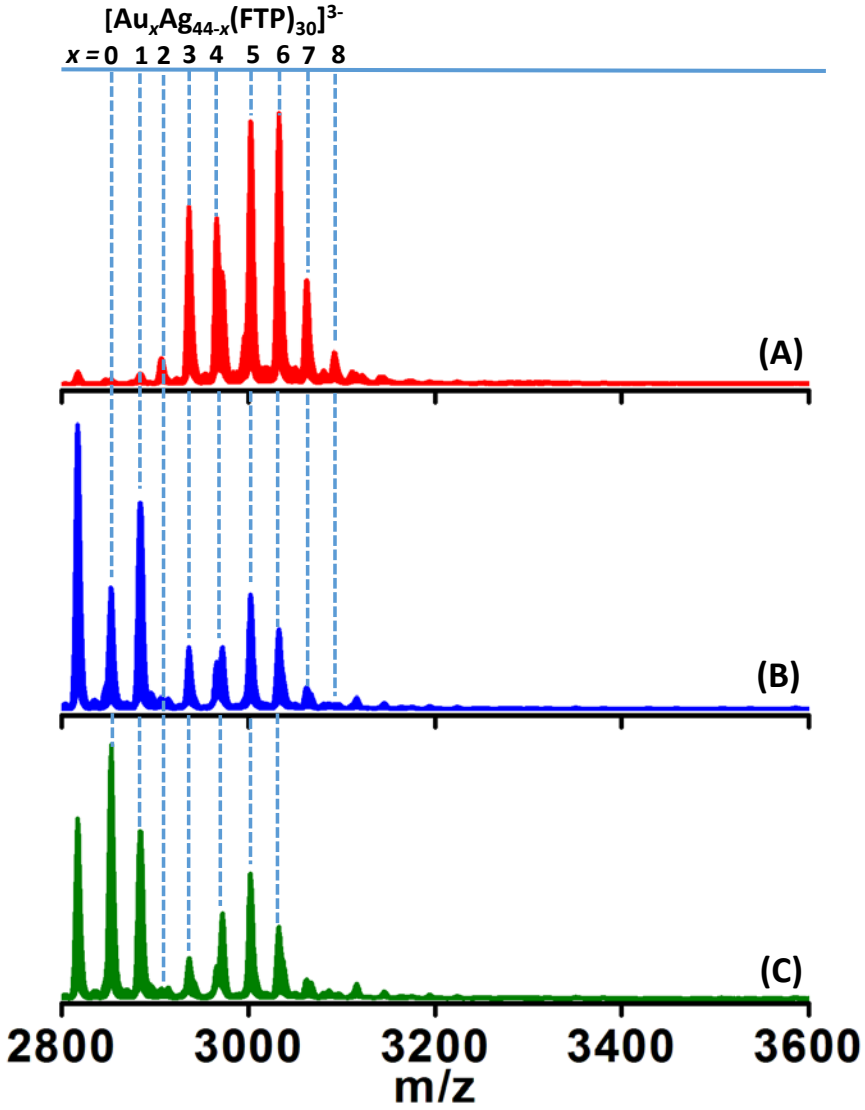

Figure S9. ESI mass spectra of a mixture of $Au_xAg_{44-x}(FTP)_{30}$ with x = 1-9, in the 3^- charge state, before (A), 2 min (B) and 1.0 h (C) after the addition of $Ag_{44}(FTP)_{30}$ into it.

Supporting Information 10

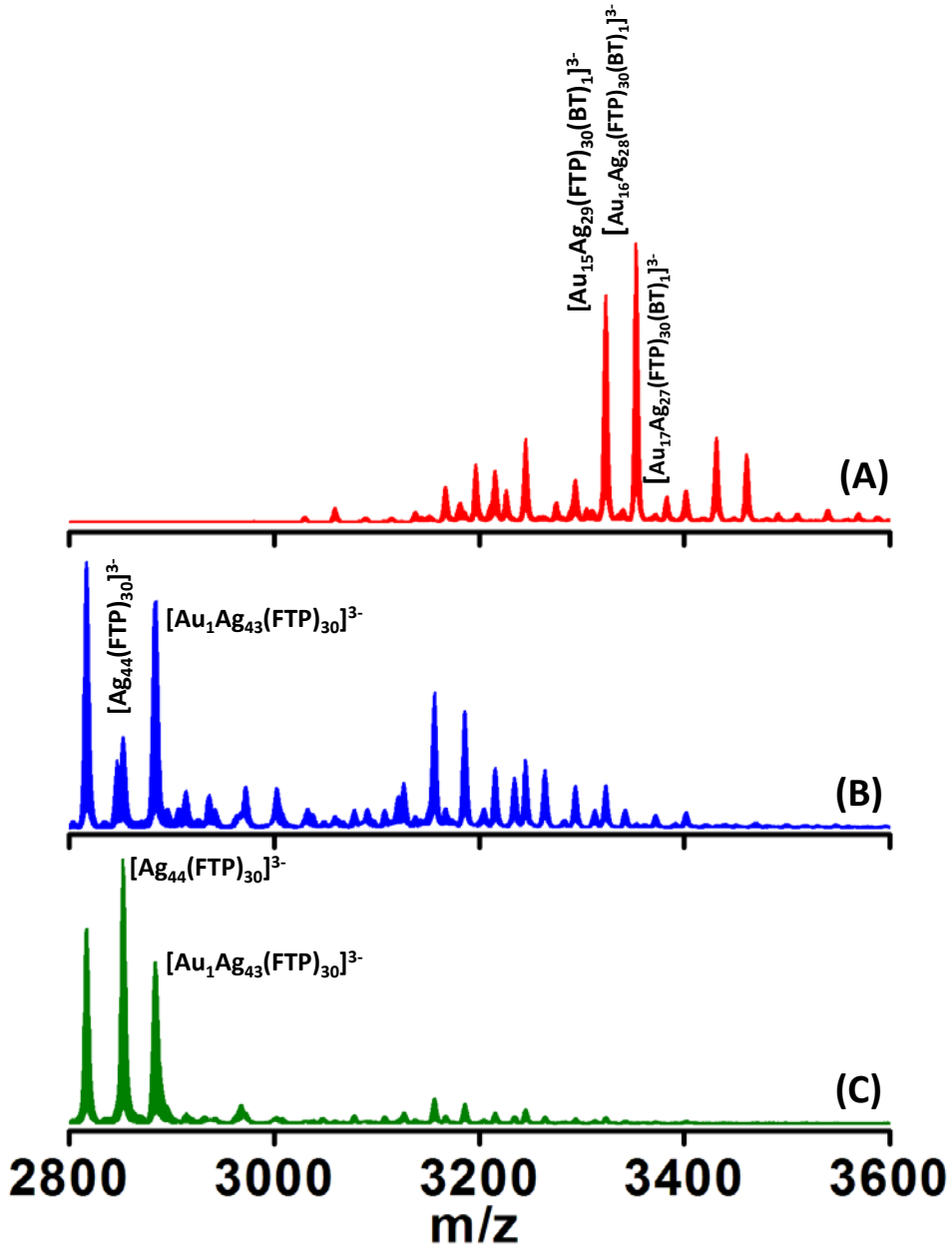

Figure S10. ESI mass spectra of a mixture of $Au_xAg_{44-x}(FTP)_{30}$ with x > 12 before (A), 2 min (B), 1.0 h (C) after the addition of $Ag_{44}(FTP)_{30}$ into it. Comparison of the mass spectra shown in (A)-(C) reveals that the intensity of the $Au_xAg_{44-x}(FTP)_{30}$ with x > 12 decreased significantly and $Au_xAg_{44-x}(FTP)_{30}$ with x < 12 appeared with significantly higher in intensity after the addition of $Ag_{44}(FTP)_{30}$ into it. These observations confirm that Au atoms of $Au_xAg_{44-x}(FTP)_{30}$ with x > 12 can be substituted with Ag atoms of $Ag_{44}(FTP)_{30}$ to form $Au_xAg_{44-x}(FTP)_{30}$ with x < 12. The mass spectra shown in Figure S11 further confirm this conclusion.

Supporting Information 11

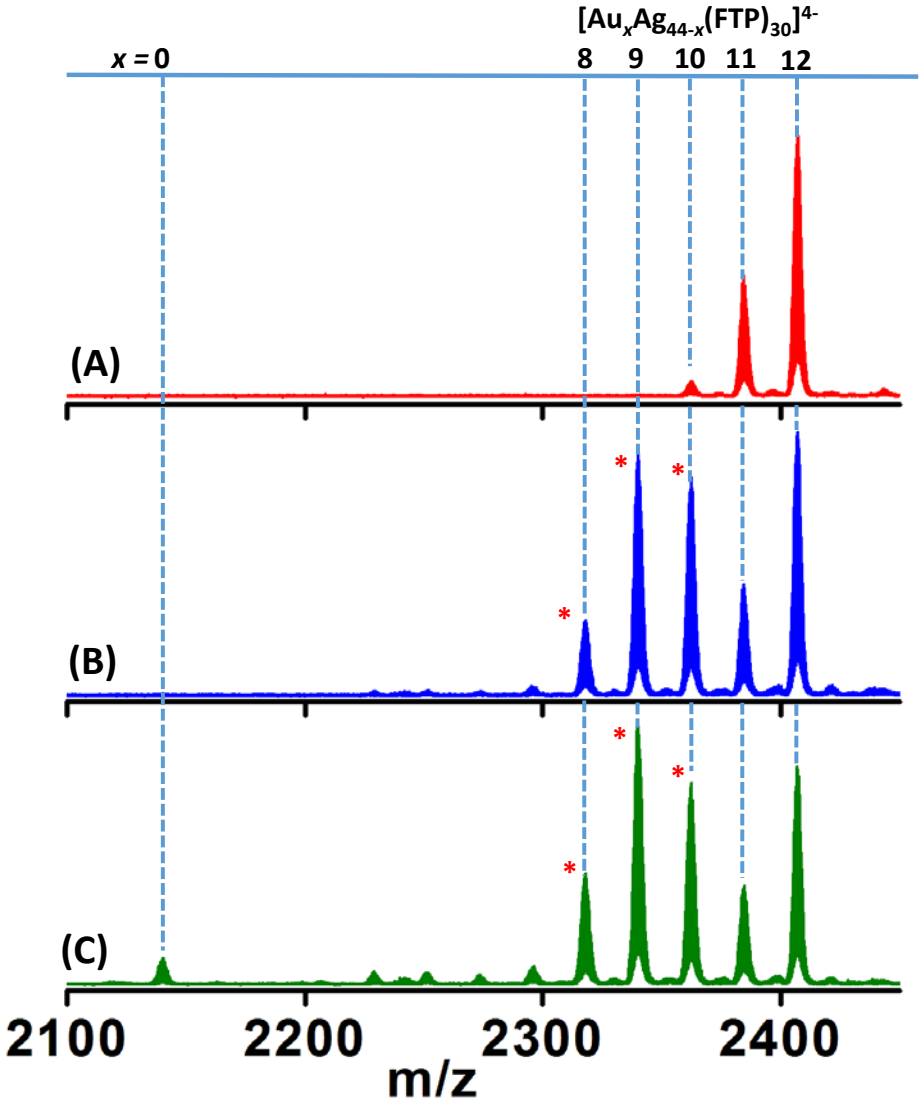

Figure S11. ESI mass spectra of a mixture of $Au_xAg_{44-x}(FTP)_{30}$ with x > 12 before (A), 2 min (B), 1.0 h (C) after the addition of $Ag_{44}(FTP)_{30}$ into it. Note that $Au_xAg_{44-x}(FTP)_{30}$ with x > 12 do not appear in the 4^- charge state; they appear only in the 3^- charge state (see Ref. 36 in the main manuscript). Hence clusters with x > 12 were not observed in this mass spectra. Comparison of the mass spectra shown in (A)-(C) reveal that more $Au_xAg_{44-x}(FTP)_{30}$ clusters with x < 12 (labeled with *) appeared after the addition of $Ag_{44}(FTP)_{30}$ into a mixture containing $[Au_{11}Ag_{33}(FTP_{)30}]^{4-}$ and $[Au_{12}Ag_{32}(FTP)_{30}]^{4-}$. Therefore, we conclude that the additional

$Au_xAg_{44-x}(FTP)_{30}$ clusters with $x < 12$ (labeled with *) are formed from the substitution of Au atoms of $Au_xAg_{44-x}(FTP)_{30}$ clusters with $x > 12$.